energies

MDPI

Article

Integrated Optimal Design of Permanent Magnet Synchronous Generator for Smart Wind Turbine Using Genetic Algorithm

Henda Zorgani Agrebi [1], Naourez Benhadj [2], Mohamed Chaieb [3], Farooq Sher [4,*], Roua Amami [5], Rafik Neji [2] and Neil Mansfield [4]

1 Department of Electrical Engineering, National School of Engineering of Gabes, University of Gabes, Gabes 6029, Tunisia; henda.zorganiagrebi@enis.tn
2 Department of Electrical Engineering, National School of Engineering of Sfax, University of Sfax, Soukra Sfax 3036, Tunisia; naourez.benhadj@enis.tn (N.B.); rafik.neji@enis.tn (R.N.)
3 Department of Electrical Engineering, National School of Engineering of Carthage, University of Tunis, Tunis 2035, Tunisia; Mohamed.chaieb@enicarthage.rnu.tn
4 Department of Engineering, School of Science and Technology, Nottingham Trent University, Nottingham NG11 8NS, UK; Neil.Mansfield@ntu.ac.uk
5 Higher Institute of Agricultural Sciences, University of Sousse, Chott Meriem 4042, Tunisia; roua.amami1991@gmail.com
* Correspondence: Farooq.Sher@ntu.ac.uk; Tel.: +44-(0)115-84-86679

Abstract: In recent years, the investment in the wind energy sector has increased in the context of producing green electricity and saving the environment. The installation of small wind turbines (SWTs) represents an actual strategy for meeting energy needs for off-grid systems and certain specialized applications. SWTs are more expensive per kilowatt installed as compared to large-scale wind turbines. Therefore, the main objective of this study is to produce an economical technology for the wind power market offering low-cost SWTs. The idea consists of considering a simple structure of the wind turbine using direct-drive permanent magnet synchronous generator (DDPMSG). DDPMSGs are the most useful machines in the wind energy field thanks to several advantages, such as elimination of noise and maintenance cost due to suppression of the gearbox and absence of the rotor circuit excitation barriers by the presence of the permanent magnets (PMs). Their major downside is the high cost of active materials, especially the PMs. Thus, the improvement of the generator design is treated as being the main component of the considered chain to assure active materials' mass and cost reduction. The methodology studied aims to explain the approach of the design integrated by optimization of the considered system. It is based on the elaboration of analytical models to find a feasible structure for the system, taking into account the multi-disciplinary analysis. The relevance of these models is validated by the finite element method using 2D MATLAB-FEMM simulation. The models are integrated to elaborate the optimization problem based on a genetic algorithm to improve the cost of the proposed generator by minimizing the mass of its active constructive materials. As an outcome, an optimal solution is offered for the wind generators market, providing a 16% cost reduction.

Keywords: renewable energy; small wind turbine; wind energy; direct drive permanent magnet synchronous generator; finite element analysis; optimization and genetic algorithm

Citation: Agrebi, H.Z.; Benhadj, N.; Chaieb, M.; Sher, F.; Amami, R.; Neji, R.; Mansfield, N. Integrated Optimal Design of Permanent Magnet Synchronous Generator for Smart Wind Turbine Using Genetic Algorithm. *Energies* **2021**, *14*, 4642. https://doi.org/10.3390/en14154642

Academic Editor: Mario Marchesoni

Received: 11 June 2021
Accepted: 25 July 2021
Published: 30 July 2021

1. Introduction

With a rapid growth in global energy needs and facing the problem of climate and ecological change on the planet [1], the installation of wind turbines is considered nowadays as a reliable solution for electricity development [2,3]. The International Energy Agency (IEA) affirms that electricity consumption from wind power underwent a boom in the latest thirteen years, from 3.4 TWh in 1990 to 790 TWh in 2016. Moreover, the statistics provided by the World Wind Energy Association (WWEA) show that the installation of wind turbines

reached 744 GW in 2020, providing 7% of the global electricity demand. According to the report of the Global Wind Energy Council (GWEC), experts highlighted the major role of wind energy in green electricity production and announced that the year 2021 is decisive to confront barriers threatening the world evolution in the future, especially carbon emission. Without denying the importance of large-scale wind turbines in power production, small wind turbines (SWTs) gained renewed attention from manufacturers [4], creating a lucrative market thanks to their key role in off-grid installation, such as islands, rural zones and urban regions, and specialized equipment including radar, pumping station, electrification and camping-cars [5,6]. Despite their importance in energetic transition towards energy systems, SWTs are more expensive per KW compared to high-power wind turbines [5,7]. The main cause of this problem is the low interest of developed nations who are more interested in large wind turbines [5].

In fact, these small machines have received a high level of research to improve their cost per installed kilowatt. Technological and operational aspects that limit SWTs performance and electricity costs have been studied to identify the tendencies and topics that inhibit SWTs markets [8]. A techno-economic feasibility study of SWTs was carried out in the valley of Mexico Metropolitan to discuss the economic strategy that promotes the penetration of SWTs technology [9]. Optimization of power and levelized cost for shrouded SWTs was realized as presenting an average 59% decrease for the levelized cost of energy and a 74% increase in annual energy production for wind lens turbines [10]. Economic and energetic analysis of a 10 KW wind turbine were performed in two cities, Tehran and Manjil, discussing the cost of the generated electricity [11]. An overview of the SWTs market in Brazil took into account lessons learned from the American market by discussing the economic problem of these small machines to encourage the growth of this low-carbon technology [12]. The examination of energy productivity and economic viability of SWTs in South Africa has been considered to tackle the obstacles leading to the slow growth of this technology [13]. Rezza [14] treated the technical and economic analyses of home energy management systems including SWT.

In this way, from a design point of view, the European Wind Energy Association (EWEA) mentioned the necessity of improving some components of SWT to offer an effective and economical technology, while respecting the system feasibility [15]. Thus, particular regard is given to the optimal design of a direct drive permanent magnet synchronous generator (DDPMSG) as part of a simplified structure of a wind conversion chain. The objective is to decrease the mass of the active material, especially for the permanent magnets (PMs) on account of their high price [16,17]. As a result, the cost of the generator could be reduced, guaranteeing excellent reliability–performance compromise. Furthermore, various generators are used in the wind power conversion chain, such as squirrel cage induction generator (SCIG) [18,19], doubly-fed induction generator (DFIG) [20,21] and permanent magnet synchronous generator (PMSG) [22,23]. The choice of PMSGs is based on several advantages. They are the heart of many applications. These machines are used especially in direct-drive wind chains, with variable speeds. The gearless generators eliminate the noise problems and the maintenance costs from which wind chains suffer [17]. These benefit with high energy efficiency and provide a permanent magnetic yield in the air gap thanks to the presence of the PMs [24]. The absence of a circuit exciter reduces the maintenance costs of the generator's rotor and minimize its losses. Therefore, the temperature is lower and the efficiency of the machine is improved [25].

The design of electrical machines is complex due to constraints imposed by engineering domains such as electromagnetic, structural and thermal disciplines [26]. The design integrated by optimization (DIO) leads to improving the performance of the machine, such as material cost, mass and efficiency, considering the multi-physics aspects. The cost of the generator refers to the cost of the design. A large number of papers are devoted to the optimization of generators dedicated to wind turbines' applications. A surface-mounted permanent magnet synchronous generator used in low-power wind turbines is designed and optimized to reduce the cogging torque [27]. An optimal design of a coreless axial

permanent magnet synchronous generator is treated with the swarm optimization method to reduce the active material cost of the generator [28]. The optimal design of a radial flux permanent magnet generator with an outer rotor dedicated to wind turbines with direct drive is realized to reduce the cost of the wind turbine system while maintaining the high-efficiency characteristics [29].

There are various optimization methods divided into two main parts, the gradient-based algorithm and the intelligent optimization algorithm [30]. According to the literature, the genetic algorithm (GA) is the most popular evolutionary method of intelligent optimization algorithms in the design of electrical systems. A study on the design by optimization of airfoils related to a 20 KW power wind turbine was presented using a multi-objective GA and HARP-opt Code developed by the National Renewable Energy Laboratory (NREL) [5]. The sensitivity analysis and the design optimization of the flux switching permanent magnet motor are studied using the non-dominated sorting GA-II to improve the electromagnetic performance of the machine [31]. The optimal design of a PMSG used in a wind power conversion chain is elaborated based on the GA method to maximize the annual energy input and minimize the volume of the PMs in the considered generator [32]. The optimization of the total cost of the distribution network is investigated using the GA method to minimize the power losses and maximize the voltage profile [33]. An optimization method of the generator structure and control dedicated for SWT power plant according to the annual wind speed is described using the GA [34]. An approach for the design by optimization of DDPMSGs inserted in small wind turbines is realized using a multi-objective GA coupled to the fast finite element analysis (FEA) to evaluate the electromagnetic torque and the field distribution [35]. An optimization method based on the GA is interested in the auxiliary damping control with the reactive power loop on the rotor side converter of a doubly-fed induction generator used for wind farm applications [36].

In the present study, a DIO approach for PMSG's design is envisaged. The purpose of the study is two-fold. First, effective analytical models of PMSG are elaborated to find a feasible structure for the generator according to specifications drawn up by the designer. The modelling concerns radial flux PMSGs' with surface magnets and inner rotor topologies. This step is critical as the structural modelling phase represents 5% of the cost of the total design activity and also fixes 75% of the costs incurred over the life of the system [37]. Subsequently, generator information including parameters and performance are provided to develop the optimization model. On the other hand, a GA code is formulated presenting 8 mixed optimization variables and 6 constraints. Taking into account the multi-physical nature of the system (thermal-mechanical-electrical and magnetic disciplines), the target of the design by optimization of the generator is mono-objective. It aims to minimize the mass of its active components (iron, copper and especially PMs). Then, the cost of the constructive materials is reduced. The theoretical problem posed is supported by simulation results that validate the used approach. Indeed, according to the literature, the electromagnetic design analysis of the PMSG has obtained three main kinds of analysis methods: analytical method, magnetic circuit method and finite element method [30,38]. These analyses fix the thermal structural material and multi-physics aspects of the system. The FEA is the best technique producing accurate results, despite the long analysis time [38]. For the studied case, a FEA using the 2D MATLAB-FEMM software (MATLAB R2014a, FEMM 4.2) is the fundamental stage presented in the work that validates the elaborated analytical models for the PMSG design. For the optimization part, optimized output characteristics of the considered PMSG are provided according to the results of the evolutionary optimization approach (GA). As the outgrowth, an economical solution of the new lightweight PMSG is finely studied and offered to the SWTs market.

2. Multi-Physics Models of Permanent Magnet Synchronous Generator

The studied wind turbine presented in Figure 1 represents a simplified structure of the small wind conversion chains. It is devoted to remote system application and for activities in the agriculture sector (pumping station, desalination, etc.), the tourist

sector (camping cars, boats, etc.) and for certain applications (rural electrification, radars, telecommunications, etc.). It is composed of three blades with a horizontal axis coupled directly to a PMSG, delivering energy into a battery through a diode bridge. The wind is the primary source of energy that stimulates the turbine to turn. It specifies the operating condition and phenomena applied to the blades to generate the turbine power. The kinetic wind power is transferred to the gearless generator through two stages. It undergoes a variation according to the capacity of the blades to capture the energy and the mechanical losses of the turbine rotor.

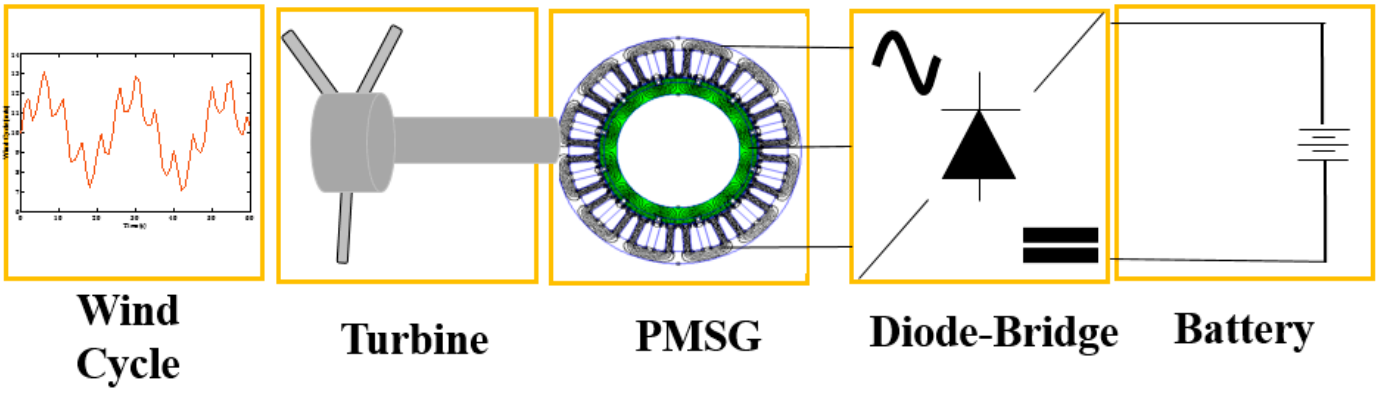

Figure 1. Simplified wind power conversion chain studied.

Being the main component of the wind power system, the cost of the generator is important. For this reason, this study is focused on the economic study of a wind generator. The PMSG studied is a radial-flux internal rotor generator using surface PMs of the Neodymium Iron Boren (NdFeB) type. Radial-flux PMSG is preferred for a wide range of speeds [25]. They are slightly more efficient and require slightly less active materials than axial-flux PMSGs [25]. For the surface magnets, they offer a simple construction for the rotor design.

This section aims to elaborate analytical models for the design of electrical PMSGs. In effect, to meet the exigency of wind generators, the competence to model their performance is of vital importance. The study mainly concerns the modelling through the examination of the multi-disciplinary system behaviour including structural, magnetic, electrical and losses models. This stage provides information about the generator parameters' calculation to produce a feasible schema according to the design specifications. The performance of the elaborated models is requested for the development of the optimization model. As a result, an initial stator and rotor design, air gap model, coil model and magnet model permit the initial design of the machine.

2.1. Structural Model

The structural characteristics of the generator are clarified in Figure 2. The principle of the geometry determination procedure is based on fixing the generator electromagnetic torque, T_{em} on its nominal value. Once the torque is fixed, the bore radius, r_s, is deduced. Then, all machine dimensions are obtained referring to the analytical model proposed in the study. Equation (1) shows a relationship between the bore radius and the electromagnetic torque [39].

$$r_s = \left(T_{em} \frac{R_{rl}}{R_{dr}} \frac{1}{\pi J_s B_{1a} K_r K_{b1}} \right)^{\frac{1}{4}} \quad (1)$$

where R_{rl} is the ratio of the bore radius, r_s, and the generator active length, l_r, R_{dr} is the ratio of the depth slot, d_s, and the bore radius, r_s, J_s represents the surface density of the current (A/m^2), B_{1a} corresponds to the magnet fundamental peak value (T), k_r is the slot

filling coefficient and k_{b1} is the winding factor. The active length of the machine, l_r, is deduced from the empirical Equation (2) [39].

$$l_r = \frac{r_s}{R_{rl}} \tag{2}$$

The air gap of the machine, g, is calculated from Equation (3) as follows [39].

$$g = 0.001 + 0.003\sqrt{r_s l_r} \tag{3}$$

The angular width of the magnet per pole, w_m, and its thickness, l_m, are deduced using the fundamental magnet properties mentioned below in Equations (4) and (5) [39].

$$w_m = \frac{2\,\alpha_{magnet}}{p}\, r_s \tag{4}$$

$$l_m = K_c g\, \frac{\mu_r}{B_r/B_a - 1} \tag{5}$$

where α_{magnet} is the magnet angle (rad), p represents the number of pole pairs, K_c shows the crankcase coefficient, B_r is the magnet remanent induction (T), B_a is the induction magnet peak value (T) and μ_r is the magnet relative permeability equal to 1.05.

For reasons of simplification of the process, the stator and rotor depth, d_y and d_r, are taken equally by assumptions, which is the same case for the tooth and slot width, w_s and w_T. These parameters are calculated using Equations (6) and (7) [39].

$$d_y = d_r = \frac{r_s\, B_a}{p\, B_y}\, \alpha_{magnet} \tag{6}$$

$$w_s = w_T = \frac{4\pi r_s}{3N_{slots}} \tag{7}$$

where B_y corresponds to the induction of the stator yoke (T) and N_{slots} is the slots' number. The slot shape is trapezoidal, having a depth, d_s, defined by Equation (8) [40].

$$d_s = R_{dr} r_s \tag{8}$$

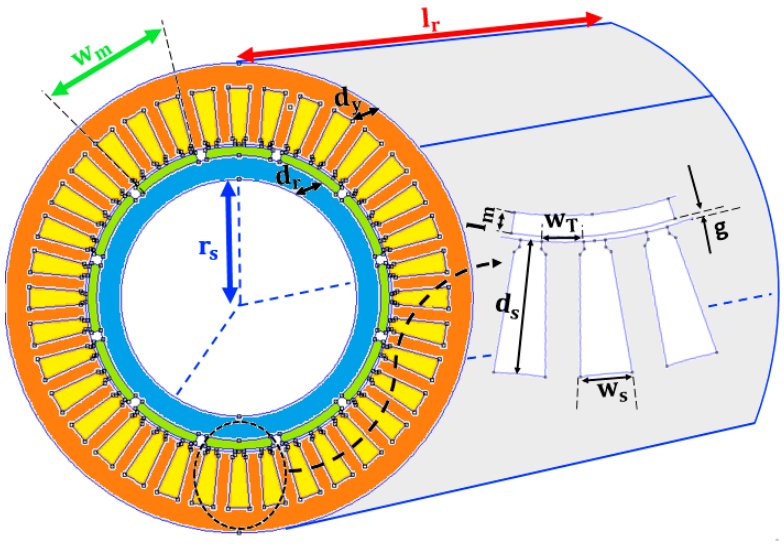

Figure 2. Permanent magnet synchronous generator structural model.

2.2. Magnetic Model

The structural parameters' values intervene in the calculation of the magnetic graders. The induction magnet peak value in the air gap, B_a, is expressed as a function of the

remanent induction, B_r, the magnet thickness, l_m, the magnet relative permeability, μ_r, the crankcase coefficient, k_c, and the air gap thickness, g, as provided by Equation (9) [39].

$$B_a = B_r \frac{l_{m/\mu_r}}{K_c\, g + l_{m/\mu_r}} \tag{9}$$

The vacuum magnetic flux received by a stator phase, Φ_s, is expressed in Equation (10) [40].

$$\Phi_s = 2N_{cs}K_{b1}N_{spp}B_{1a}r_s l_r \tag{10}$$

where N_{cs} is the conductors' number per slot and N_{spp} is the slot number per pole and per phase.

2.3. Electrical Model

The variation of the magnetic flux over time generates the birth of an electromotive force (EMF), E (V), in the 3 phases of stator windings. For the case of the studied machine, the winding distribution of the three phases is of the distributed type. The expression of the induced EMF is provided in Equation (11) [39].

$$E = p\Omega\Phi_s \tag{11}$$

where Ω is the rotation angular speed of the rotor (rad/s). The generated current, I_s (A), is obtained from the current density, J_s. It is determined using Equation (12) [40].

$$I_s = \frac{J_s d_s K_r \pi r_s}{6pN_{spp}N_{cs}} \tag{12}$$

The induced EMF in the three stator phases, $e_i(t)$ (i = 1, 2, 3), generates the presence of an induced current, $i_i(t)$, assumed sinusoidal. Therefore, there will be the presence of electromagnetic torque, $T_{em}(t)$, as shown in Equation (13) [39].

$$T_{em}(t) = \frac{e_1(t)i_1(t) + e_2(t)i_2(t) + e_3(t)i_3(t)}{\Omega} \tag{13}$$

2.4. Losses Model and Generator Efficiency

In this section, the losses model is explained at first. Generator losses are divided into 3 categories, these are mechanical losses, P_m, iron losses, P_f, and Joule losses, P_j.

Mechanical losses are due to the friction coefficient of the machine, f_m, when rotating the rotor with an angular speed Ω. The expression of the mechanical losses, P_m, is expressed as follows [39].

$$P_m = f_m\Omega^2 \tag{14}$$

Being a magnetic material, the generator iron losses, P_f, are localized in the teeth and the stator yoke. The formula of the iron losses is provided in Equation (15) [39].

$$P_f = 4f[V_{teeth}{B_d}^2\left(\frac{\alpha_p}{\Delta_{tt}} + K_{h2}\right) + V_{yoke}{B_y}^2(\frac{\alpha_p}{\Delta_{ty}} + K_{h2})] \tag{15}$$

where f is the frequency of the establishment of the induction in the material, V_{teeth} is the teeth volume, V_{yoke} is the stator yoke volume, B_d is the maximum induction in the teeth (T), B_y is the induction in the stator yoke (T), K_{h2} and α_p are characteristic coefficients of the material used (for sheet metal of FeSi NO20, K_{h2} = 52 Am/(V.s), α_p = 0.06 Am/V), Δ_{tt} is the time required in the magnet extremity for the induction to pass through a tooth at the rotational angular speed and Δ_{ty} is the induction build-up in the stator yoke. The Joule

losses, P_j, are resulted from the temperature rising from the stator resistors traversed by currents. Its expression is shown in Equation (16) [39].

$$P_j = 3R_s{I_s}^2 \tag{16}$$

where R_s is the phase resistance (Ω). On the other hand, the generator efficiency, η, is defined in Equation (17) as being the ratio between the generator useful power, P_u, and the power it absorbs from the turbine power, P_w [41].

$$\eta = \frac{P_u}{P_w} = \frac{P_w - P_m - P_f - P_j}{P_w} \tag{17}$$

The useful power, P_u, is obtained based on different losses generated during the generator operation. Figure 3 represents the power balance at the level of the wind generator. It shows the various losses of the system during the energy transfer. Wind power is the input variable of the system, which stimulates its operation. It generates the mechanical rotational movement of the turbine shaft, leading to mechanical losses, P_m. The direct transmission of the turbine torque to the generator rotor creates an electromagnetic torque producing Joule losses, P_J, at the stator iron losses, P_f, in the ferromagnetic material.

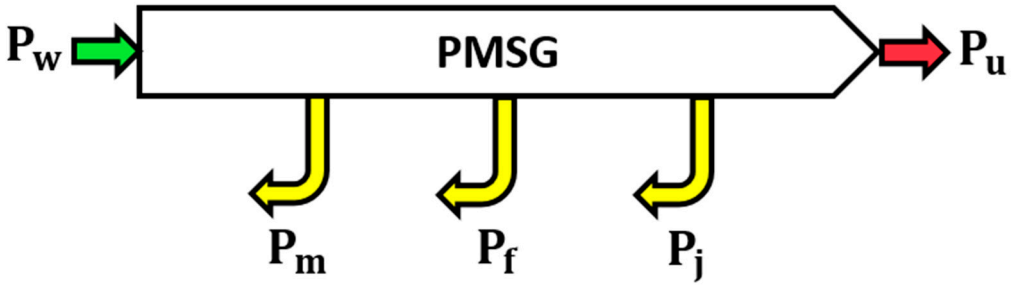

Figure 3. Permanent magnet synchronous generator power balance.

3. Design Integrated by Optimization of PMSG

The design of electrical machines becomes more and more complex as more engineering domains and constraints are developed. The design integrated by optimization (DIO) permits to produce an optimal design while respecting specifications and technological-physical requirements. The DIO represents two parts, the design model with analysis method and design optimization with algorithms. Design modelling, as presented in Section 2, provides effective models to develop the optimization model, the second stage of the DIO. The main object of the optimization part is to improve the qualifications of the studied generator. In effect, despite their popularity across many applications, the major drawback of the PMSG is the high cost of constructive materials, especially for the NdFeB PMs. Thus, the formulation of the optimization problem is elaborated to generate a lightweight prototype, resulting in the reduced cost of the system. In this framework, the optimization model is treated with the GA method, which is described in Figure 4. The GA uses a vocabulary adopted from that of natural genetics.

GA represents an evolutionary process similar to that of the Darwin model. The process begins with the generation of an initial random population of individuals. These individuals, points of the state space, adopt the value of the criterion to be optimized. The passage from one generation to another goes through the stages of selection, crossing and mutation to be able to generate a new population for the next generation. The evaluation of the fitness function makes it possible to provide optimal solutions of the generations considered until reaching a unique optimal solution imposed by a condition of convergence of the iterative system. Two parameters of the probability of application of genetic operators are defined: crossing rate, r_c, and mutation rate, r_m. At this stage, the formulation of the

problem consists of establishing the object of the optimization, optimization variables and the constraints.

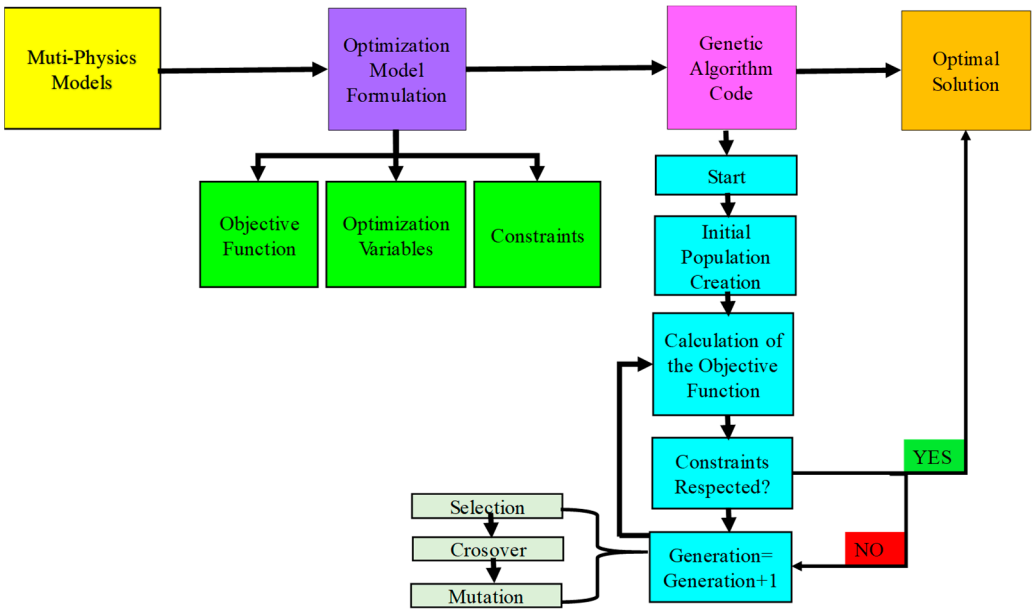

Figure 4. Steps of the design by optimization approach using the genetic algorithm method.

3.1. Objective Function

The objective of the design optimization is to minimize the mass of the generator's active parts, which leads to reduce its cost. Therefore, it is a single criteria optimization with 8 mixed variables and 6 constraints. The objective function also called the fitness function, $F_{fitness}$, corresponds to the function calculating the generator mass, as provided in Equation (18) [39].

$$F_{fitness} = 2\pi\rho_{iron} l_r d_y (2r_s + d_s - g - l_m) + \rho_{iron} l_r N_{slots} S_{tooth} + \rho_{copper}\, S_{u\_Slot} N_{slots} (l_r + l_{w.head}) + 2\pi K_p \rho_{magnet}\, l_r l_m (r_s - g - \tfrac{l_m}{2}) \quad (18)$$

where ρ_{iron} is the density of the iron, ρ_{copper} is the density of the copper, S_{u_Slot} is the useful area of the slot, $l_{w.head}$ is the winding head length and ρ_{magnet} is the density of the magnet.

3.2. Optimization Variables

The optimization variables considered in this study are the input design variables used during the generator sizing phase. The variation range of these parameters is determined according to the expertise of the design. The design variables are made of 6 continuous variables and 2 discrete variables, as indicated in Table 1.

Table 1. Type and variation range of the optimization variables.

Optimization Variables	Symbol	Unit	Type	Range
Ration of the slot depth to the bore radius of the machine	R_{dr}	_	Continuous	[0.03, 3]
Ratio of the bore radius to the active length of the machine	R_{rl}	_	Continuous	[0.1, 5]
Pole pairs number	P	_	Discrete	[1, . . . , 30]
Current surface density	J_s	A/mm^2	Continuous	[0.5, 4]
Slot number per pole and per phase	N_{spp}	_	Discrete	[1, . . . , 5]
Rated power	P_r	W	Continuous	[300, 3000]
Rated angular rotation speed	Ω_r	rad/s	Continuous	[25, 95]
Induction in the stator yoke	B_y	T	Continuous	[1.2, 1.8]

3.3. Design Constraints

The design constraints intervene during the variation of the optimization variables in their field of exploration in order to guarantee the feasibility of the system. For the case studied, 6 constraints are taken into consideration. The first, highlighted in Equation (19), requires that the number of conductors per slot, N_{cs}, should be greater than 1.

$$N_{cs} \geq 1 \tag{19}$$

The second, presented in Equation (20), discuss the slot capability to accommodate all conductors per slot to complete the winding. Therefore, the area reserved for a conductor per slot must be greater than a minimum value, S_{c_min}, equal to 0.5 mm^2.

$$\frac{S_{slot}}{N_{cs}} \geq S_{c\_min} \tag{20}$$

The third, shown in Equation (21), concerns the slot width, which must be considered to avoid having too-thin slots, which annoy the windings generator. Thereby, the slot width must be greater than a minimum width of a slot w_{s_min}, typically equal to 4 mm.

$$w_s \geq w_{s\_min} \tag{21}$$

The fourth declared in Equation (22), discuss the problem of magnets' demagnetization during generator operation. This constraint requires that the maximum induction produced by the stator currents, B_s, must not exceed the difference between the peak value of the permanent magnet induction, B_a, and the demagnetization induction of the magnet, B_d. The induction at the stator level, B_s, is expressed by Equation (23) as a function of the geometric quantities [39].

$$B_s \geq B_a - B_d \tag{22}$$

$$B_s = \frac{3\mu_0 N_{spp} N_{cs} I_s}{K_c g + l_m/\mu_r} \tag{23}$$

where μ_0 represents the space permeability equal to 1.25 H/m.

The fifth, mentioned in Equation (24), insists that the stator windings' temperature, T_{ws}, must not override the maximum temperature value of the insulating T_{im}. In the case of the studied machine, a class F winding is used with a maximum temperature of 155 °C.

$$T_{ws} \geq T_{im} \tag{24}$$

The final constraint, as expressed in Equation (25), guarantees the maximum energy efficiency provided by the generator. It is fixed greater than or equal to 0.9. The maximum value of the efficiency is calculated according to the evolution and the convergence of the optimization problem.

$$\eta \geq 0.9 \tag{25}$$

4. Design Simulation Integrated by Optimization of PMSG

The results obtained from the DIO approach represents two parts: the design modelling results at the basis of the FEA and the design optimization results based on the GA method.

4.1. Finite Element Analysis of the Elaborated PMSG Analytical Models

The pertinence of the analytical models of the PMSG is requested. The most popular method available to evaluate machines' parameters is the finite element method (FEM) [38]. The FEM method permits solving the complexity of the electromagnetic field [42]. It permits to accurately calculate the electromagnetic parameters such as torque power and flux and also allows the design to be evaluated according to several criteria. Therefore, in this phase, a MATLAB-FEMM code is developed. This code, using the LUA script

language of octave FEMM 4.2 via a set of MATLAB functions, allows the design of electrical machines in 2D and studies their electromagnetic behaviour especially with respect to the magnet material saturation. This code requires as input parameters geometric graders and some properties of the machine. The goal of this part is to evaluate the relevance of the developed analytical models on a reference machine while respecting the performance and the constraints of the system. A method of simulation using the FEM by FEMM software is used and considered as a reliable method to treat the electromagnetic behaviour of an outer rotor permanent magnet brushless DC motor for torque improvement [42]. In fact, referring to an existing external rotor PMSG in our laboratory that can be used in the same small wind sector, the fixed input parameters are taken as shown in Table 2.

Table 2. Input parameters of an external PMSG dedicated for small wind power applications.

Parameters	Symbol	Unit	Value
Ratio of the slot depth to the bore radius of the machine	R_{dr}	_	0.366
Ratio of the bore radius to the active length of the machine	R_{rl}	_	2.025
Pole pairs number	P	_	6
Current surface density	J_s	A/mm^2	2.7
Slot number per pole and per phase	N_{spp}	_	1
Rated power	P_r	W	1100
Rated angular rotation speed	Ω_r	rad/s	40
Induction in the stator yoke	B_y	T	1.4

The topology of the studied generator differs from the topology of the reference machine. It represents a surface permanent magnet generator with radial flux and an internal rotor. Thereby, the design parameters associated with this generator were obtained from the structural analytical model and designed in 2D with the finite element software FEMM, as shown in Figure 5. This step requires the definition of different components (stator, rotor, air gap, slots, magnets and boundaries box), the material composing the machine (Steel 1010 for the stator and rotor yoke, NdFe30 for the magnets, coils for the slots) and measuring of dimensions and thickness in each part.

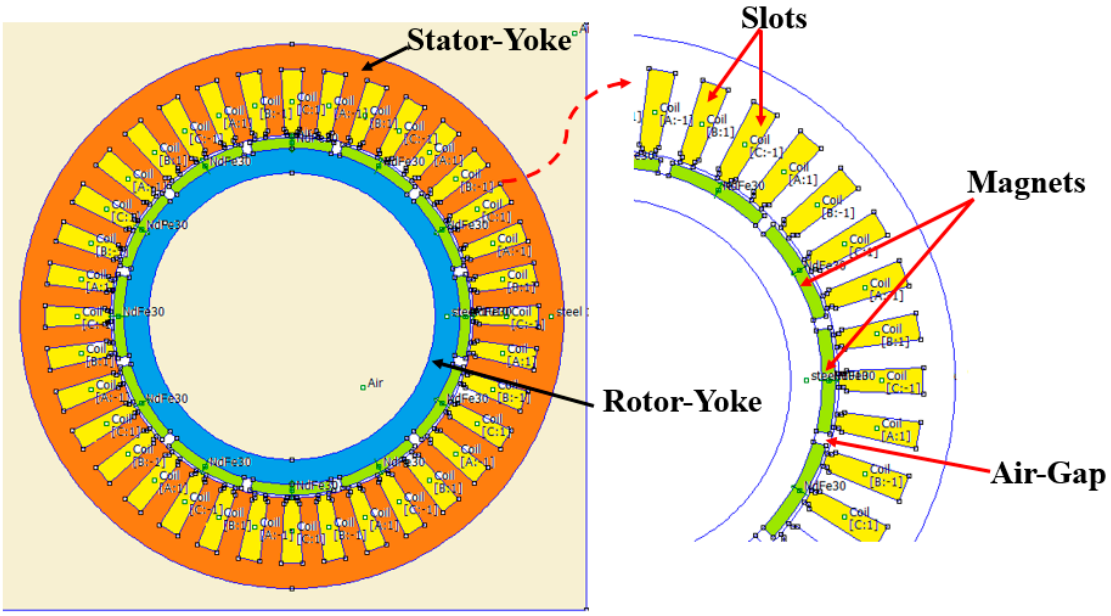

Figure 5. Permanent magnet synchronous generator structure with the 2D finite element analysis software, FEMM.

The FEA by FEMM is a part of a cross-sectional discredited engine into a small volume, called mesh or finite element. The 2D mesh of the active parts of the machine is shown

in Figure 6. It generates an efficient mesh using a triangle in the critical region (air gap and the stator and rotor yoke) to accommodate between the time of simulation and the accuracy of results. According to Gerber et al. [43], the mesh generation using triangle is the most powerful method of mesh because of its various advantages. The air gap mesh is too small due to the complexity of the electromagnetic field. For other regions, the mesh is bigger due to the simplicity of the electromagnetic field. The rotor is turned with a step chosen by the designer to obtain the mechanical variation of the electromagnetic field. The smaller the step, the more precise the values. The simulation results were obtained with a rotational angle of the rotor fixed to 1° and for a mesh of 49,872 nodes.

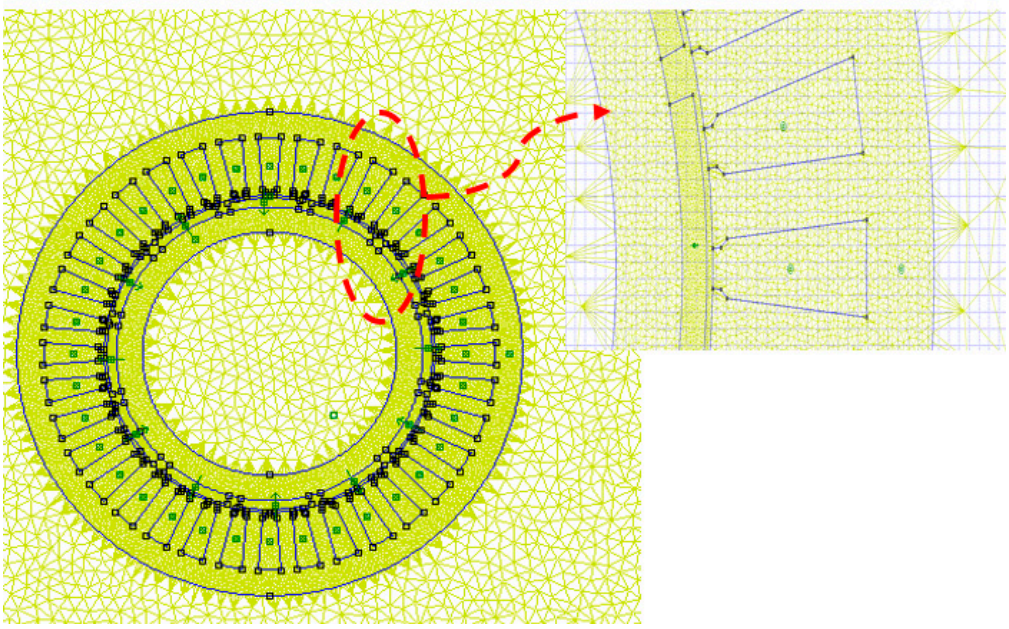

Figure 6. 2D mesh of permanent magnet synchronous generator.

The vector potential mapping and the distribution of the flux link are shown in Figure 7. It represents the best representation of the saturation phenomena within the machine. Additionally, finite element analysis in using FEMM software for an inset permanent magnet synchronous machine represents the importance of the magnetic flux density to investigate the core saturation induced in the stator and rotor of three experimental machines [44]. For the studied case, the density of the magnetic field reached approximately 1.4 T in the stator yoke and 1.7 T not only in the ribs but also in stator teeth.

The evolution of the electromagnetic graders with the finite element method is presented in Figure 8. Figure 8a shows the magnetic induction shape of the permanent magnets in the air gap, with a peak value approximately equal to 0.9 T. The variation of the magnetic flux in the three unloaded phases as a function of mechanical angle is obtained in Figure 8b. Its rate is perfectly sinusoidal, giving a peak value equal to 0.35 Wb. The variation of the magnetic flux over time generates the birth of an electromotive force in the 3 phases of stator windings, as illustrated in Figure 8c. The shape of the EMF curves presents a distortion of the sinusoid. The fast Fourier-transform of these signals is presented in Figure 8d and explains this deformation by the presence of harmonics 3 and 5. These harmonics are due to the effect of the technique's winding the robust representation of the electromagnetic phenomena analysis with the finite element method. The variation of the electromagnetic torque as a function of the mechanical angle is presented in Figure 8e. Its average value per finite element is 23.5 N·m.

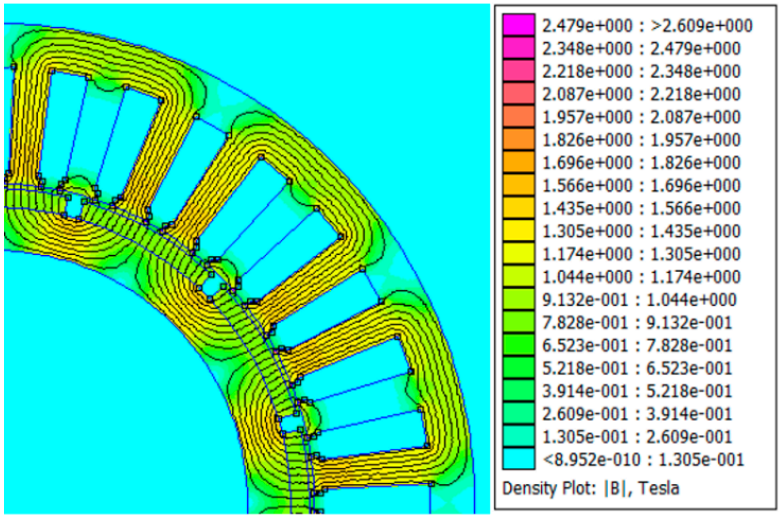

Figure 7. 2D magnetic flux density and vector potential in the permanent magnet synchronous generator.

The analytical and numerical values of the electromagnetic parameters are summarized as mentioned in Table 3. The percentage of the error rate between the results of the two models is calculated. The percentage values are tolerable. Indeed, the error presented for the case of the permanent magnets' induction and the vacuum flux is low, with percentages of 6% and 2.9% respectively. For the case of the EMFs' and the electromagnetic torque's error, the percentages of 26% and 17% respectively, are explained by the windings technique effect in the generator considered and the smoothness of a finite element approach compared to an analytical approach. In the context of an optimal design based on analytical models of a 5 MW axial-flux permanent magnet synchronous generator used for wind turbines' applications, analysis by the finite element method of the elaborated model supported by experimental validation showed a good arrangement between the studied models [45]. It affirms the relevance of the finite element method in analyzing electromagnetic graders within a machine. Therefore, the developed analytical model specialized for the PMSG's design is validated. The working method is adopted for the problem of design by optimization of the PMSG.

Table 3. Analytical results vs. numerical results of the PMSG electromagnetic graders.

Parameters	Symbol	Unit	Analytical Value	Numerical Value	Error (%)
Induction	B_a	T	0.85	0.90	6
Maximum Vacuum-Induced Flux	Φ_{m0}	Wb	0.34	0.35	2.90
Maximum Vacuum-Induced EMF	E_{m0}	V	82.50	65.50	26
Electromagnetic Torque	T_{em}	N·m	27.50	23.50	17

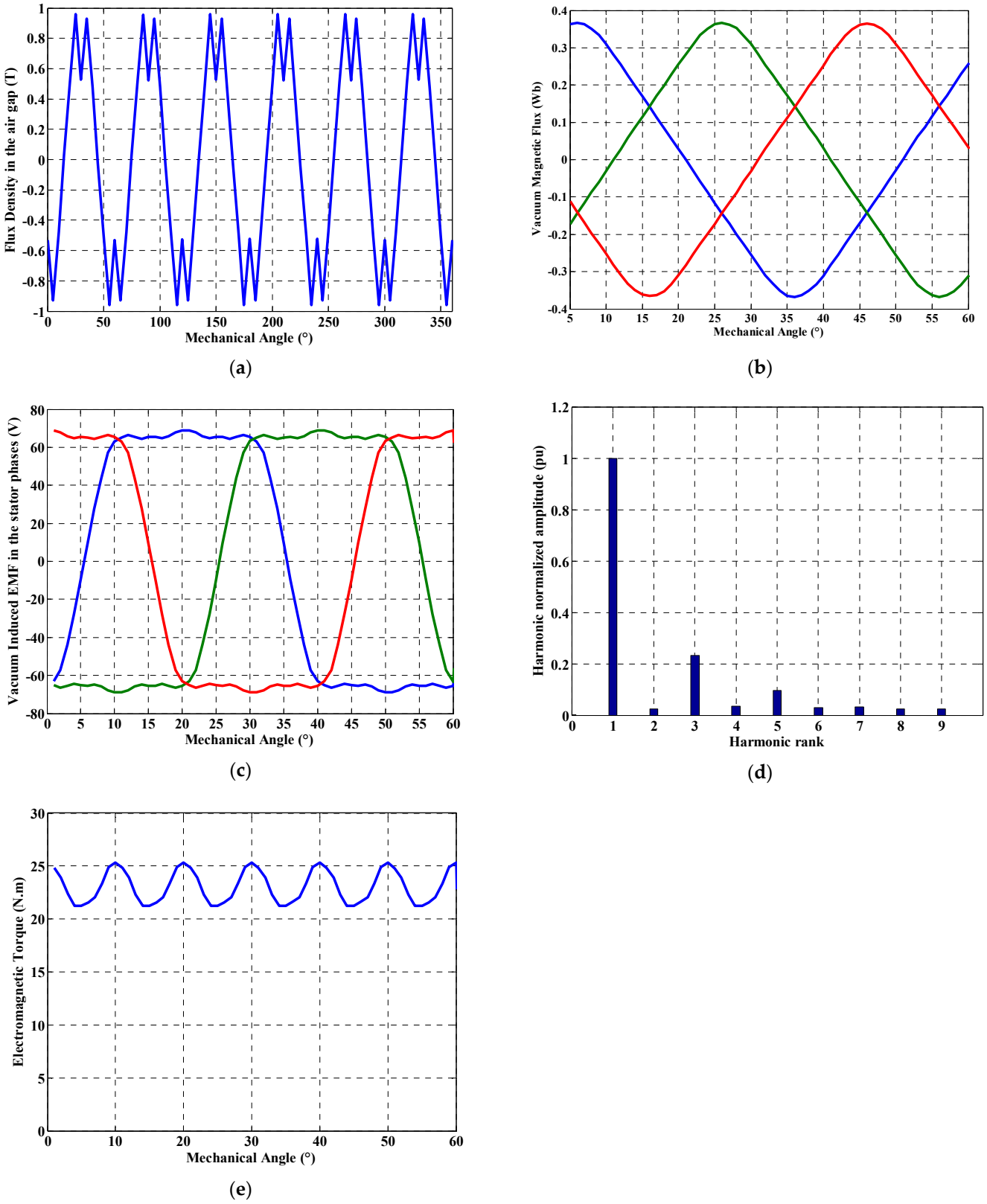

Figure 8. Finite element analysis results of electromagnetic graders within the permanent magnet synchronous generator: (**a**) flux density in air gap vs. mechanical angle, (**b**) vacuum magnetic flux vs. mechanical angle, (**c**) vacuum induced EMF in stator windings vs. mechanical angle, (**d**) fast Fourier transform (FFT) of vacuum induced EMF in stator phases and (**e**) electromagnetic torque vs. mechanical angle.

4.2. The Optimization Algorithm Simulation Results

The evolution of the GA process generates at first an initial random population of individuals adopting the value of the criterion to be optimized. Then, the creation of new generations is carried out to evaluate the objective function at each iteration, until reaching the optimal solution imposed by a condition of convergence of the iterative system. Figure 9 represents the simulation results of the GA applied for our case study. It describes the pace of the fitness function and the evolution of the optimized design parameters for the different generations. As shown in Figure 9a, the GA simulation was spread over 197 generations until it converged to the optimum mass equal to 6.26 kg. There was a weight reduction of 41% from the initial mass. There will be the birth of a new optimized machine delivering a power, P_r of 1125 W at the nominal rotation speed, Ω_r equal to 27.3 rad/s, with an efficiency, $\eta$of 94%. The characteristics of this machine are inspired by the results of the curves provided above. The main parameters of the initial and optimized PMSG are declared in Table 4. To analyze the effect of the evolution of the design parameters on the machine performance, the results of Figure 9 are considered. Increasing the number of pole pairs, p from 6 to 12 seems logical for the reduction of the stator and rotor yoke mass while they are inversely proportional. Likewise, for the induction in the stator yoke, B_y increasing its value from 1.4 to 1.8 T is acceptable for reducing the mass of the stator and rotor yoke. The decrease of the rotation angular speed, Ω, is pertinent for the augmentation of the electromagnetic torque and the reduction of the mechanical losses. However, the mass is inversely proportional to the torque, so the optimal value of Ω is logical.

Table 4. Main parameters of PMSG before and after optimization.

Parameters	Symbol	Unit	Value	
			Initial Design	Optimized Design
Bore radius	r_s	mm	83.16	121.23
Active length of the generator	l_r	mm	41.06	26.19
Total length of the generator	l_{g_tot}	mm	144.10	95.90
Stator depth yoke	d_y	mm	11.29	6.40
Rotor depth yoke	d_r	mm	11.29	6.40
Slot depth	d_s	mm	30.43	22.71
Slot width	w_s	mm	9.67	7.05
Tooth width	w_T	mm	9.67	7.05
Magnet thickness	l_m	mm	4.93	4.91
Air gap thickness	g	mm	1.17	1.16
Magnet angular width per pole	w_m	mm	36.28	26.44
Number of conductors per slot	N_{cs}	_	47	35
Number of pole pairs	p	_	6	12
Maximum vacuum-induced flux	Φ_{m0}	Wb	0.34	0.23
Maximum vacuum-induced EMF	E_{m0}	V	82.55	78
Induced current	I_s	A	4.44	4.8
Phase synchronous inductance	L_s	mH	5.25	3.43
Phase synchronous resistance	R_s	Ω	0.51	0.72

As for post-processing action after the optimization, a 2D finite element design of the optimized PMSG is elaborated based on the results in Table 4 to validate the reliability of the optimal structure. In this context, a finite element analysis of an optimized permanent magnet synchronous generator is permitted to study the harmonic distortion rate of electromagnetic graders and assure the improvement of its performance [46]. Besides, the 2D design ensures the feasibility of the structure of the solution proposed. The new conception is provided in Figure 10. It shows the safe distribution of flux links within the machine and clarifies the vector potential mapping, which asserts the unsaturation of the material.

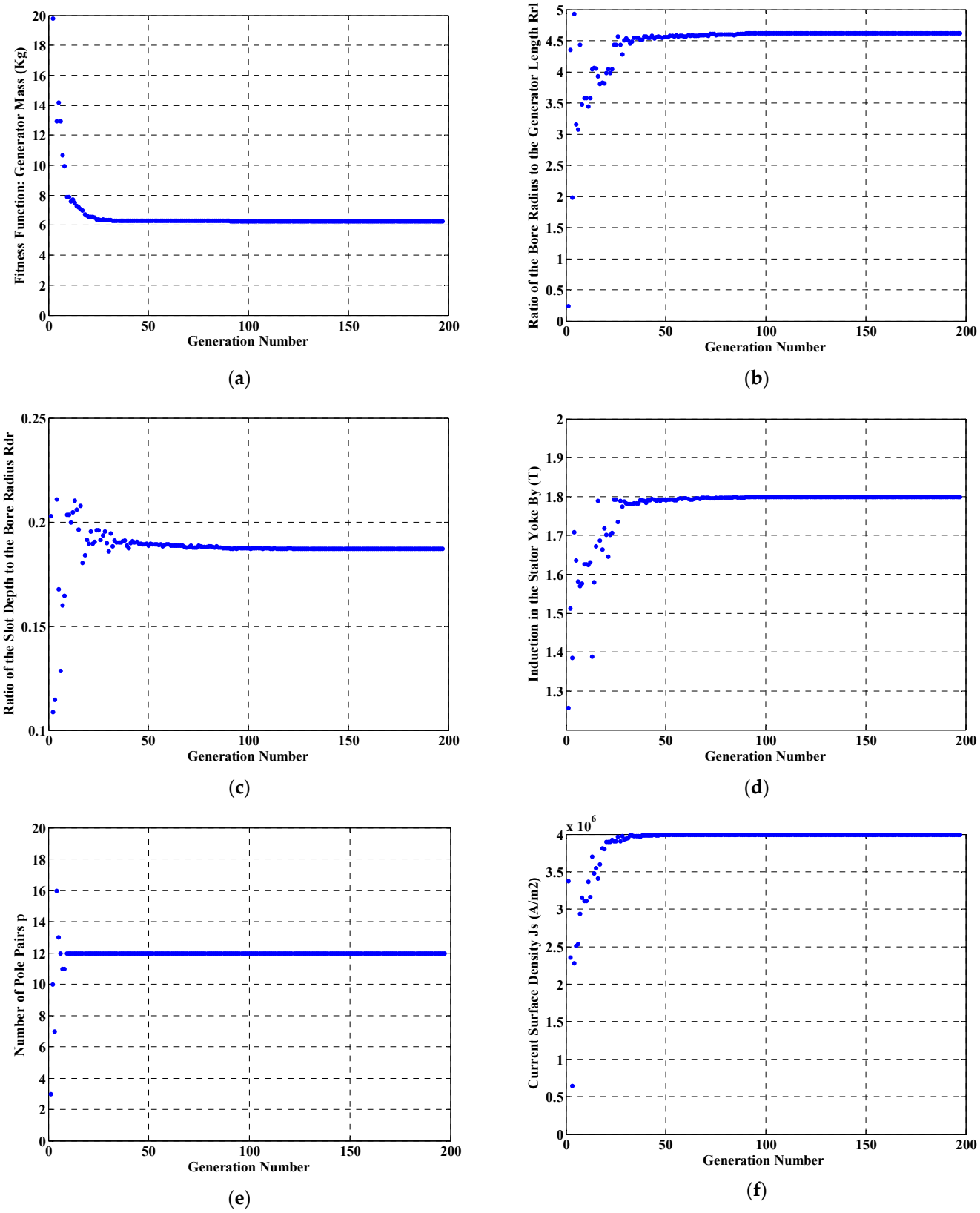

Figure 9. *Cont.*

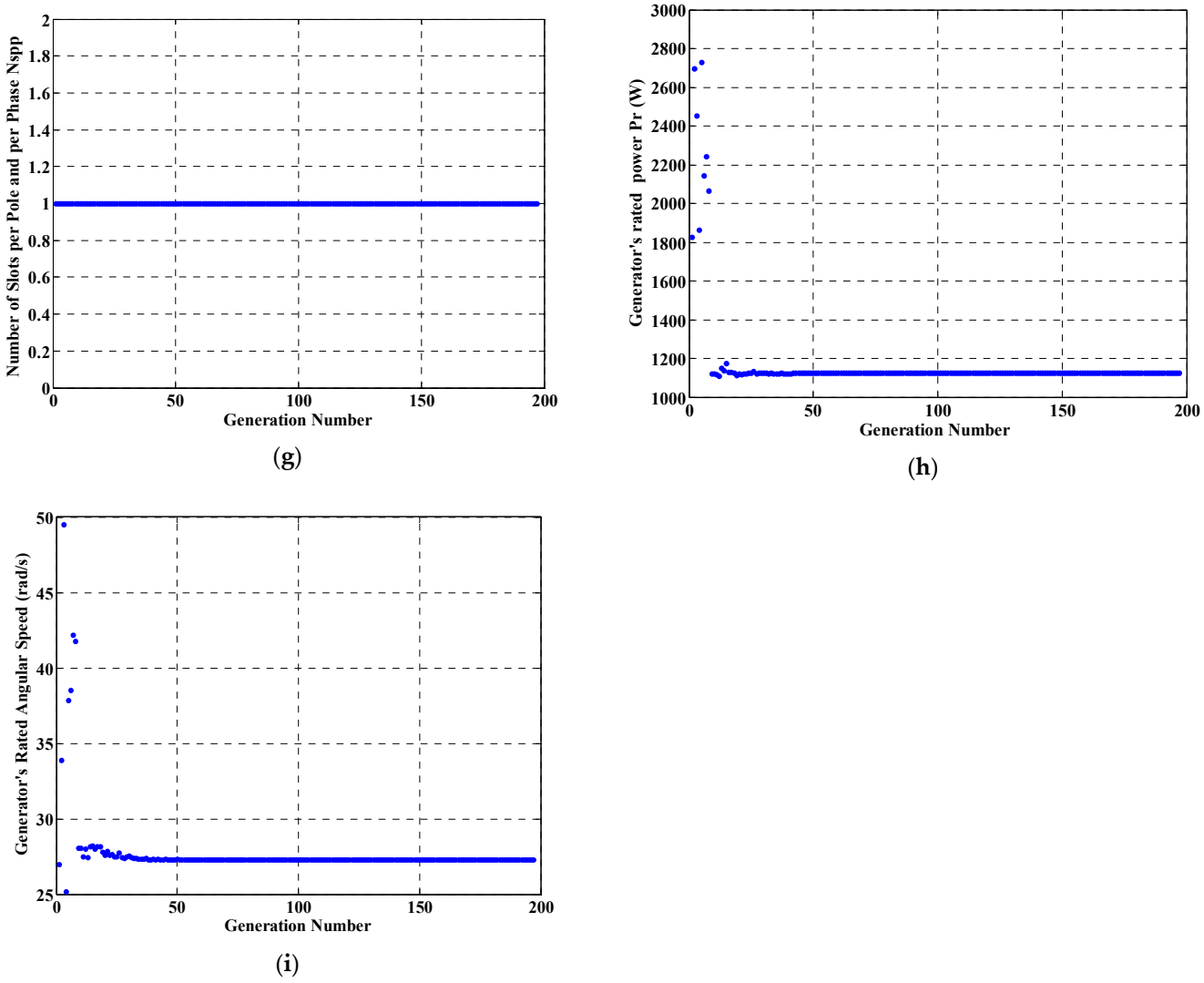

Figure 9. Simulation results of genetic algorithm optimization code: (**a**) generator's mass vs. generation number, (**b**) ratio of the bore radius to the generator's length (Rrl) vs. generation number, (**c**) ratio of the slot's depth to the bore radius (Rdr) vs. generation number, (**d**) induction in the stator yoke (B_y) vs. generation number, (**e**) number of pole pairs (p) vs. generation number, (**f**) current surface density (Js) vs. generation number, (**g**) number of slots per pole and per phase (N_{spp}) vs. generation number, (**h**) generator's rated power (P_r) vs. generation number and (**i**) generator's rated angular speed (Ω_r) vs. generation number.

From an economical point of view, the cost of the PMSG, $C_{Generator}$, refers to the sum of the active components' cost. It depends on the magnet cost per kg, C_{magnet}, the copper cost per kg, C_{Copper}, and the iron cost per kg, C_{iron}, as explained in Equation (26).

$$C_{Generator} = C_{magnet}M_{magnet} + C_{Copper}M_{copper} + C_{iron}M_{iron} \quad (26)$$

where M_{magnet} is the magnet mass (kg), M_{copper} is the copper mass (kg) and M_{iron} is the iron mass in the entire machine (kg). A comparison between the reference and the optimal PMSG from a mass and cost point of view is established in Table 5.

The iron mass of the machine is notably reduced from 7.58 to 4.06 kg. Furthermore, despite a large number of teeth and slots, the tooth surface and the slot's useful surface become smaller so that the total mass of the teeth goes from 3.19 to 1.93 kg. The stator and rotor yoke thickness are notably reduced, offering a 45% and 57% reduction weight, with an increase in the bore radius value from 0.083 to 0.121 m. The mass of copper goes from 2.43 to 1.66 kg. For the PMs, the mass varies slightly from 0.59 to 0.54 kg, offering an 8.5%

mass reduction. The PMSG's cost is reduced from 51.22 to 43.36 €, equivalent to a 16% reduction from the initial price. In fact, iron cost occupies 0.95% of the machine construction materials' total price, the copper cost reaches 21.84% and the PMs' cost represents 77.21%. As known, PMs are the most expensive component, which explains the major drawback encountered by permanent magnet machines. According to the literature, an optimal multidisciplinary design of a permanent magnet synchronous generator dedicated to a 50 KW wind turbine is realized [46], offering a reduction of 17.4% cost of system's active material to offer a low-cost wind generator. The mass of the permanent magnet is reduced by 21.4%. Furthermore, from an economical point of view, the percentages obtained in this study appear relevant.

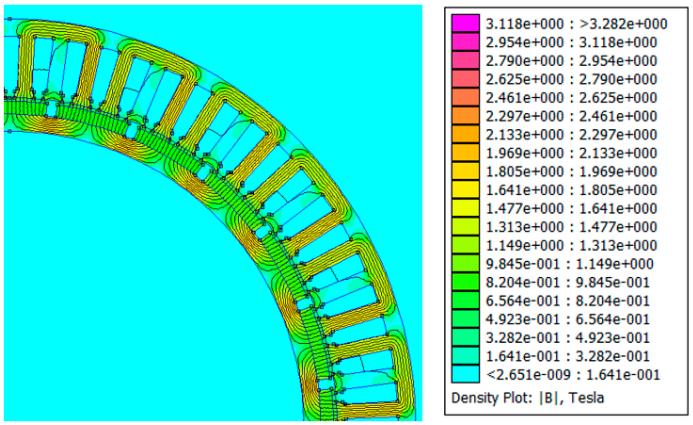

Figure 10. 2D magnetic flux density and vector potential in PMSG's optimized structure.

Table 5. The mass and cost of reference and optimized PMSG.

System Active Part	Initial Mass (kg)	Initial Cost (€)	Optimized Mass (kg)	New Cost (€)
Copper	2.43	13.87	1.66	9.47
Iron	7.58	0.77	4.06	0.41
Magnet (NdFeB)	0.59	36.58	0.54	33.48
Generator	10.6	51.22	6.26	43.36

5. Conclusions

In a context related to the production of economical technologies of small wind turbines, the design integrated by optimization of a direct drive permanent magnet synchronous generator was treated in this article as being one of the critical components of a simplified small wind turbine. This approach had a significant impact on the performance and the cost of the considered machine. In fact, this method represented two main aims. The first target was the elaboration of analytical models, including structural magnetic and electrical disciplines. The relevance of the elaborated models was analyzed by the finite element method. This analysis is required to test the performance of the generator modelling phase, which represents 5% of the cost of the total design and fixes 75% of the costs incurred over the life of the system. Therefore, by analyzing the electromagnetic graders of a reference machine dedicated to a small wind turbine with MATLAB-FEMM software, the error between analytical and numerical results was discussed. For the induction in the air gap and the vacuum magnetic flux, the error was low, with percentages of 6% and 2.9% respectively. For the vacuum induced EMF and the electromagnetic torque, the errors of 26% and 17% were explained by the distributed windings effect and the finality of the finite element method in the electromagnetic analysis of electrical machines. Consequently, the analytical models were validated and integrated into the formulation of the optimization model, the second step of the DIO. The optimization problem aimed to produce a

lightweight generator to reduce the cost of the constructive materials, especially in the case of the high cost of the NdFeB magnets. The genetic algorithm approach was cited as being the most used method in the design of electrical systems, and generated an optimal solution with 94% power efficiency, offering a mass reduction of the generator from 10.6 to 6.26 kg, equivalent to a 41% weight reduction and a 16% cost reduction. The validation of the optimized structure by finite element analysis was considered to support the reliability of the approach. As the outcome, an optimal design of the PMSG was interpreted, offering a low mass-cost configuration while respecting the feasibility and the energy efficiency of the system. As a perspective, the DIO of the entire simplified wind chain, including the airfoils and the convertor, will be an achievement in the small wind power production sector that will make small wind power generation more financially viable.

Author Contributions: Conceptualization, H.Z.A., N.B., M.C. and F.S.; Methodology, H.Z.A., R.A. and R.N.; Software, H.Z.A., N.B., N.M. and F.S.; Validation, H.Z.A. and M.C.; Formal Analysis, H.Z.A., N.B. and F.S.; Investigation, H.Z.A., R.A. and F.S.; Resources, H.Z.A., F.S. and N.M.; Data Curation, H.Z.A. and N.B.; Writing—Original Draft Preparation, H.Z.A., N.B., F.S. and R.A.; Writing—Review and Editing, H.Z.A., F.S., R.A. and N.M.; Visualization, H.Z.A., M.C., F.S. and R.N.; Supervision, F.S., R.N. and N.M.; Project Administration, M.C., F.S. and N.M.; Funding Acquisition, F.S. and N.M. All authors have read and agreed to the published version of the manuscript.

Funding: This research received no external funding.

Institutional Review Board Statement: Not applicable.

Informed Consent Statement: Not applicable.

Data Availability Statement: Not applicable.

Acknowledgments: The authors are thankful to the respective institutions for their financial support.

Conflicts of Interest: The authors declare no conflict of interest.

References

1. Ren, G.; Liu, J.; Wan, J.; Guo, Y.; Yu, D. Overview of wind power intermittency: Impacts, measurements, and mitigation solutions. *Appl. Energy* **2017**, *204*, 47–65. [CrossRef]
2. Dai, J.; Yang, X.; Wen, L. Development of wind power industry in China: A comprehensive assessment. *Renew. Sustain. Energy Rev.* **2018**, *97*, 156–164. [CrossRef]
3. Nazir, M.S.; Ali, N.; Bilal, M.; Iqbal, H.M. Potential environmental impacts of wind energy development: A global perspective. *Curr. Opin. Environ. Sci. Health* **2020**, *13*, 85–90. [CrossRef]
4. Anup, K.; Whale, J.; Urmee, T. Urban wind conditions and small wind turbines in the built environment: A review. *Renew. Energy* **2019**, *131*, 268–283.
5. Ram, K.R.; Lal, S.P.; Ahmed, M.R. Design and optimization of airfoils and a 20 kW wind turbine using multi-objective genetic algorithm and HARP_Opt code. *Renew. Energy* **2019**, *144*, 56–67. [CrossRef]
6. Akinyele, D. Techno-economic design and performance analysis of nanogrid systems for households in energy-poor villages. *Sustain. Cities Soc.* **2017**, *34*, 335–357. [CrossRef]
7. Papi, F.; Nocentini, A.; Ferrara, G.; Bianchini, A. On the Use of Modern Engineering Codes for Designing a Small Wind Turbine: An Annotated Case Study. *Energies* **2021**, *14*, 1013. [CrossRef]
8. Torres-Madroñero, J.L.; Alvarez-Montoya, J.; Restrepo-Montoya, D.; Tamayo-Avendaño, J.M.; Nieto-Londoño, C.; Sierra-Pérez, J.J.E. Technological and Operational Aspects That Limit Small Wind Turbines Performance. *Energies* **2020**, *13*, 6123. [CrossRef]
9. Rodriguez-Hernandez, O.; Martinez, M.; Lopez-Villalobos, C.; Garcia, H.; Campos-Amezcua, R.J.E. Techno-economic feasibility study of small wind turbines in the Valley of Mexico metropolitan area. *Energies* **2019**, *12*, 890. [CrossRef]
10. Khojasteh, H.; Noorollahi, Y.; Tahani, M.; Masdari, M.J.I. Optimization of Power and Levelized Cost for Shrouded Small Wind Turbine. *Inventions* **2020**, *5*, 59. [CrossRef]
11. Ehyaei, M.; Ahmadi, A.; Rosen, M.A. Energy, exergy, economic and advanced and extended exergy analyses of a wind turbine. *Energy Convers. Manag.* **2019**, *183*, 369–381. [CrossRef]
12. Chagas, C.C.M.; Pereira, M.G.; Rosa, L.P.; da Silva, N.F.; Freitas, M.A.V.; Hunt, J.D. From megawatts to kilowatts: A review of small wind turbine applications, lessons from the US to Brazil. *Sustainability* **2020**, *12*, 2760. [CrossRef]
13. Olatayo, K.I.; Wichers, J.H.; Stoker, P.W. Energy and economic performance of small wind energy systems under different climatic conditions of South Africa. *Renew. Sustain. Energy Rev.* **2018**, *98*, 376–392. [CrossRef]
14. Hemmati, R. Technical and economic analysis of home energy management system incorporating small-scale wind turbine and battery energy storage system. *J. Clean. Prod.* **2017**, *159*, 106–118. [CrossRef]

15. Bazzo, T.d.P.M.; Kölzer, J.F.; Carlson, R.; Wurtz, F.; Gerbaud, L. Multiphysics design optimization of a permanent magnet synchronous generator. *IEEE Trans. Ind. Electron.* **2017**, *64*, 9815–9823. [CrossRef]
16. Shen, Y.; Zhu, Z. Analysis of electromagnetic performance of Halbach PM brushless machines having mixed grade and unequal height of magnets. *IEEE Trans. Magn.* **2012**, *49*, 1461–1469. [CrossRef]
17. Gardner, M.C.; Jack, B.E.; Johnson, M.; Toliyat, H.A. Comparison of surface mounted permanent magnet coaxial radial flux magnetic gears independently optimized for volume, cost, and mass. *IEEE Trans. Ind. Appl.* **2018**, *54*, 2237–2245. [CrossRef]
18. Satpathy, A.S.; Kastha, D.; Kishore, N. Vienna Rectifier Fed Squirrel Cage Induction Generator based Stand-alone Wind Energy Conversion System. *IEEE Trans. Power Electron.* **2021**, *36*, 10186–10198. [CrossRef]
19. da Silva Santos, M.; Barros, L.S. Offshore wind energy conversion system based on squirrel cage induction generator connected to the grid by VSC-HVDC link. In Proceedings of the 2019 IEEE PES Innovative Smart Grid Technologies Conference-Latin America (ISGT Latin America), Gramado, Brazil, 15–18 September 2019; pp. 1–6.
20. Zhang, J.; Cui, M.; He, Y. Robustness and adaptability analysis for equivalent model of doubly fed induction generator wind farm using measured data. *Appl. Energy* **2020**, *261*, 114362. [CrossRef]
21. Mazouz, F.; Belkacem, S.; Colak, I.; Drid, S.; Harbouche, Y. Adaptive direct power control for double fed induction generator used in wind turbine. *Int. J. Electr. Power Energy Syst.* **2020**, *114*, 105395. [CrossRef]
22. Ahmad, G.; Amin, U. Design, construction and study of small scale vertical axis wind turbine based on a magnetically levitated axial flux permanent magnet generator. *Renew. Energy* **2017**, *101*, 286–292. [CrossRef]
23. Vaimann, T.; Kudrjavtsev, O.; Kilk, A.; Kallaste, A.; Rassolkin, A. Design and prototyping of directly driven outer rotor permanent magnet generator for small scale wind turbines. *Adv. Electr. Electron. Eng.* **2018**, *16*, 271–278. [CrossRef]
24. Zhao, X.; Niu, S.; Fu, W. Sensitivity analysis and design optimization of a new hybrid-excited dual-PM generator with relieving-DC-saturation structure for stand-alone wind power generation. *IEEE Trans. Magn.* **2019**, *56*, 1–5. [CrossRef]
25. Sindhya, K.; Manninen, A.; Miettinen, K.; Pippuri, J. Design of a permanent magnet synchronous generator using interactive multiobjective optimization. *IEEE Trans. Ind. Electron.* **2017**, *64*, 9776–9783. [CrossRef]
26. Bramerdorfer, G.; Tapia, J.A.; Pyrhönen, J.J.; Cavagnino, A. Modern electrical machine design optimization: Techniques, trends, and best practices. *IEEE Trans. Ind. Electron.* **2018**, *65*, 7672–7684. [CrossRef]
27. Öztürk, N.; Dalcalı, A.; Celik, E.; Sakar, S. Cogging torque reduction by optimal design of PM synchronous generator for wind turbines. *Int. J. Hydrog. Energy* **2017**, *42*, 17593–17600. [CrossRef]
28. Daghigh, A.; Javadi, H.; Torkaman, H. Optimal design of coreless axial flux permanent magnet synchronous generator with reduced cost considering improved PM leakage flux model. *Electr. Power Compon. Syst.* **2017**, *45*, 264–278. [CrossRef]
29. Abdoos, A.; Moazzen, M.E.; Ebadi, A. Optimal Design of a Radial-Flux Permanent Magnet Generator with Outer-Rotor for Direct-Drive Wind Turbines. *Comput. Intell. Electr. Eng.* **2020**, *11*, 51–64.
30. Lei, G.; Zhu, J.; Guo, Y.; Liu, C.; Ma, B. A review of design optimization methods for electrical machines. *Energies* **2017**, *10*, 1962. [CrossRef]
31. Mahmouditabar, F.; Vahedi, A.; Mosavi, M.R.; Bafghi, M.H. Sensitivity analysis and multiobjective design optimization of flux switching permanent magnet motor using MLP-ANN modeling and NSGA-II algorithm. *Int. Trans. Electr. Energy Syst.* **2020**, *30*, e12511. [CrossRef]
32. Faiz, J.; Ebrahimi, B.M.; Rajabi-Sebdani, M.; Khan, A. Optimal design of permanent magnet synchronous generator for wind energy conversion considering annual energy input and magnet volume. In Proceedings of the 2009 International Conference on Sustainable Power Generation and Supply, Nanjing, China, 6–7 April 2009; pp. 1–6.
33. Syahputra, R. Distribution network optimization based on genetic algorithm. *J. Electr. Technol. UMY* **2017**, *1*, 1–9. [CrossRef]
34. Wrobel, K.; Tomczewski, K.; Sliwinski, A.; Tomczewski, A.J.E. Optimization of a Small Wind Power Plant for Annual Wind Speed Distribution. *Energies* **2021**, *14*, 1587. [CrossRef]
35. Palmieri, M.; Bozzella, S.; Cascella, G.L.; Bronzini, M.; Torresi, M.; Cupertino, F.J.E. Wind Micro-Turbine Networks for Urban Areas: Optimal Design and Power Scalability of Permanent Magnet Generators. *Energies* **2018**, *11*, 2759. [CrossRef]
36. Zhao, B.; Li, H.; Wang, M.; Chen, Y.; Liu, S.; Yang, D.; Yang, C.; Hu, Y.; Chen, Z.J.E. An optimal reactive power control strategy for a DFIG-based wind farm to damp the sub-synchronous oscillation of a power system. *Energies* **2014**, *7*, 3086–3103. [CrossRef]
37. Dogan, H. Méthodologie de Conception des Machines Synchrones à Aimants. Application au Véhicule éLectrique Avec Chargeur Rapide Embarqué. Ph.D. Dissertation, Université de Grenoble, Grenoble, France, 2013.
38. Lee, J.H.; Song, J.-Y.; Kim, D.-W.; Kim, J.-W.; Kim, Y.-J.; Jung, S.-Y. Particle swarm optimization algorithm with intelligent particle number control for optimal design of electric machines. *IEEE Trans. Ind. Electron.* **2017**, *65*, 1791–1798. [CrossRef]
39. Tran, D.H. *Conception Optimale Intégrée d'une Chaîne Éolienne "Passive": Analyse de Robustesse, Validation Expérimentale*; Institut National Polytechnique de Toulouse-INPT: Toulouse, France, 2010.
40. Abdelli, A. Optimal design of an interior permanent magnet synchronous motor for wide constant-power region operation: Considering thermal and electromagnetic aspects. *SAE Int. J. Altern. Powertrains* **2014**, *3*, 129–138. [CrossRef]
41. Tran, D.H.; Sareni, B.; Roboam, X.; Bru, E.; Andrade, A.D. Robust design of a passive wind turbine system. *COMPEL: Int J Comput. Maths. Electr. Electron. Eng.* **2012**, *31*, 932–944. [CrossRef]
42. Kumaravelu, U.D.; Mohamed Yakub, S.J.M.; Engineering, S. Simulation of outer rotor permanent magnet brushless DC motor using finite element method for torque improvement. *Model. Simul. Eng* **2012**, *2012*, 961212. [CrossRef]

43. Gerber, S. *A Finite Element Based Optimisation Tool for Electrical Machines*; University of Stellenbosch: Stellenbosch, South Africa, 2011.
44. Ling, J.M.; Nur, T.J. Influence of edge slotting of magnet pole with fixed slot opening width on the cogging torque in inset permanent magnet synchronous machine. *Adv. Mech. Eng.* **2016**, *8*, 1687814016659598. [CrossRef]
45. Hemeida, A.; Sergeant, P.; Rasekh, A.; Vansompel, H.; Vierendeels, J. An optimal design of a 5MW AFPMSM for wind turbine applications using analytical model. In Proceedings of the 2016 XXII International Conference on Electrical Machines (ICEM), Lausanne, Switzerland, 4–7 September 2016; pp. 1290–1297.
46. Bazzo, T.P.M. *Conception Optimale Multidisciplinaire de Générateurs Synchrones à Aimants Permanents Pour Éoliennes Tenant Compte de la Courbe D'occurrence du Vent*; Universidade Federal de Santa Catarina: Florianópolis, Brazil, 2017.